International Journal of ENGINE RESEARCH

Special Issue Article

International J of Engine Research
2015, Vol. 16(3) 474–484
© IMechE 2014
Reprints and permissions:
sagepub.co.uk/journalsPermissions.nav
DOI: 10.1177/1468087414552616
jer.sagepub.com
SAGE

Real-time internal residual mass estimation for combustion with high cyclic variability

J Larimore[1], E Hellström[1], S Jade[1], AG Stefanopoulou[1] and Li Jiang[2]

Abstract

In this work, a physics-based method of estimating the residual mass in a recompression homogeneous charge compression ignition engine is developed and analyzed for real-time implementation. The estimation routine is achieved through in-cylinder pressure and exhaust temperature measurements coupled with energy and mass conservation laws applied during the exhaust period. Experimental results on a multicylinder gasoline homogeneous charge compression ignition engine and dynamic analysis demonstrate the estimation routine's ability to perform across a wide range of operating conditions as well as on a cycle-by-cycle basis for highly variable combustion phasing data.

Keywords

Homogeneous charge compression ignition, residual gas fraction

Date received: 30 April 2014; accepted: 12 August 2014

Introduction

Autoignition timing control in homogeneous charge compression ignition (HCCI) combustion requires careful regulation of the temperature, pressure and composition of the pre-combustion cylinder charge.[1,2] The regulation of charge properties is carried out in recompression HCCI by retaining a large fraction of the post-combustion residual gases before they can be exhausted[3,4] in addition to controlling the fuel injection timing.[5–7] Accurate modeling of the residual gas fraction is important due to HCCI's high sensitivity to the thermal energy associated with the residual gases.[8–11] If too much residual mass is trapped, the charge temperature is too high and combustion occurs very early causing a loss in efficiency and potential engine damage.[12] If too little mass is trapped, the combustion becomes very late and oscillatory.[13,14] In the latter case, excess oxygen and unburned fuel can cause heat release during recompression which can result in efficiency loss, misfires, torque fluctuations and potential engine damage may occur.

Due to this sensitivity, it is desirable to estimate the residual gas fraction online. There have been several methods described in the literature[15–18] for offline estimation of the residual mass for steady-state conditions. This work presents a method of residual estimation which is computationally simple enough to be implemented online while still maintaining a physical basis and alleviating the need of steady-state conditions. Analysis of the algorithm demonstrates fast convergence and the capability to handle high variability data. Furthermore, a sensitivity analysis is provided which indicates that a tuning parameter can be used to affect the dynamics and convergence of the algorithm. A block diagram of how the method works with respect to cycle events is given in Figure 1.

The article is outlined as follows: first, an offline residual estimation technique is presented in section "Iterative estimation." In section "Real-time estimation" the method of section "Iterative estimation" is modified for transients and online implementation. In section "Dynamic analysis," an analysis of the algorithm is performed to demonstrate its convergence properties and sensitivities. In section "Experimental results and setup," the experimental setup is explained

[1]Department of Mechanical Engineering, University of Michigan, Ann Arbor, MI, USA
[2]Robert Bosch LLC, Denham, UK

Corresponding author:
J Larimore, Department of Mechanical Engineering, University of Michigan, 3479 Burbank Dr. Ann Arbor, MI 48105, USA.
Email: larimore@umich.edu

Downloaded from jer.sagepub.com at UNIV OF MICHIGAN on February 18, 2016

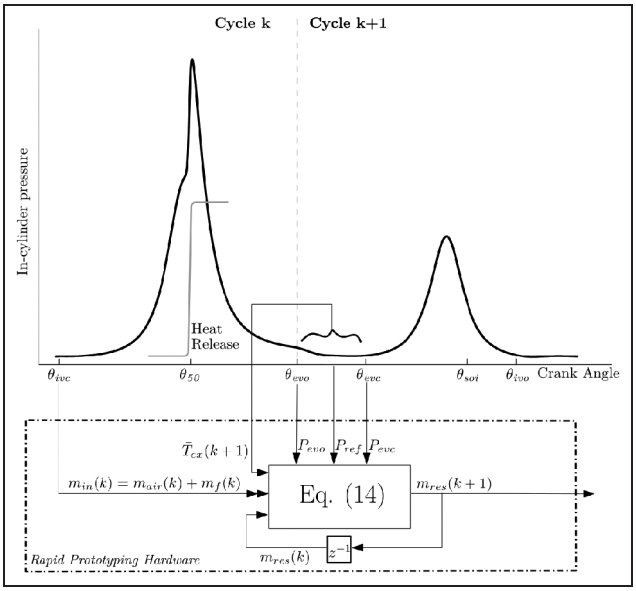

Figure 1. A block diagram representation of the inputs and outputs of the online residual mass estimation.

and the experimental results are provided; conclusions are drawn in section "Conclusion."

Residual mass estimation

Crucial for proper combustion analysis is the determination of residual mass. In section "Iterative estimation," we derive an algorithm for trapped internal residual mass in an engine operating with negative valve overlap (NVO), following the method of Fitzgerald et al.[15] Additionally, a modification to allow for highly variable data, as outlined in Larimore et al.,[19] is presented. This method is suitable for offline analysis. Furthermore, the formulation is modified to minimize the effects of steady-state assumptions and simplify the algorithm for real-time implementation in section "Real-time estimation."

Iterative estimation

The trapped residual mass (m_{res}) is defined as the in-cylinder charge at the time of exhaust valve closing (EVC) and is based on the ideal gas law $m_{res} = P_{evc}V_{evc}/RT_{evc}$. The in-cylinder pressure is measured, which provides P_{evc} and the cylinder volume at EVC, V_{evc}, is known. The gas constant is for a burned gas composition and is assumed constant and known, $R = 290(\mathrm{J/kg\,K})$. Therefore, to determine the residual mass, T_{evc} must be estimated. To do so, a system of equations is developed from which T_{evc}, and consequently m_{res}, may be determined.

In steady-state conditions, the mass flowing out of the cylinder during the exhaust stroke, m_{out}, is equal to mass of fresh air and fuel, m_{air} and m_f, respectively, inducted into the cylinder within a given cycle

$$m_{out} = m_{air} + m_f = m_{in} \tag{1}$$

The mass that leaves through the exhaust process (exhaust valve opening (EVO) → EVC) can be described as

$$\frac{P_{evo}V_{evo}}{RT_{evo}} - \frac{P_{evc}V_{evc}}{RT_{evc}} = m_{air} + m_f \tag{2}$$

where the pressures at the valve events, P_{evo} and P_{evc}, are measured, as are m_{air} and m_f. Equation (2) has two unknowns, T_{evo} and T_{evc}; therefore, an additional relation is needed to solve for the unknown temperatures.

In addition to the steady-state conservation of mass in equation (2), the exhaust process can be approximated by an ideal gas undergoing a reversible process. The heat loss per unit mass, during the crank angle interval $\theta_0 \rightarrow \theta_1$, is given by

$$q_l(\theta_0, \theta_1) = \int_{T(\theta_0)}^{T(\theta_1)} c_p dT - R \int_{P(\theta_0)}^{P(\theta_1)} \frac{T}{P} dP \tag{3}$$

where c_p is the specific heat of the exhaust gas which is assumed constant and known. The exhaust process is split into two parts, a blowdown phase and compression phase. The ratio of the heat losses for these two phases is denoted by r_{ex}

$$r_{ex} = \frac{q_l(\theta_{evo}, \theta_{ref})}{q_l(\theta_{ref}, \theta_{evc})} \tag{4}$$

The point used to split the exhaust process, θ_{ref}, is referred to as the reference point. In Fitzgerald et al.,[15] it is the point when exhaust runner pressure is equal to 1 atm. To accommodate boosted conditions, one could instead use the point of minimum pressure as in Hellström et al.[20] However, in highly variable conditions, the minimum could occur close to the valve events. For example, it was observed that the minimum may be at EVO following misfires, see Figure 2. To avoid possible numerical issues associated with this scenario, the reference point is fixed in the middle of the valve open period, $\theta_{ref} = (\theta_{evo} + \theta_{evc})/2$.

By combining equations (3) and (4), with simplifications from Fitzgerald et al.,[15] we arrive at the equation

$$\begin{aligned} &(c_p + a)T_{evo} + (c_p - b)r_{ex} \\ &T_{evc} = T_{ref}\big(c_p - a + (c_p + b)r_{ex}\big) \end{aligned} \tag{5}$$

where $a = 1/2R \log P_{ref}/P_{evo}$ and $b = 1/2R \log P_{evc}/P_{ref}$. The variables T_{ref} and P_{ref} are the measured exhaust gas temperature and in-cylinder pressure at θ_{ref}, respectively.

The heat loss ratio r_{ex} is estimated by convective heat transfer to the walls as governed by

$$\frac{dQ_l}{dt} = Ah_c(T_{cyl} - T_w) \tag{6}$$

where the heat transfer coefficient, h_c, is determined using the Woschni method from Heywood,[21] and A is the cylinder area. A constant wall temperature, T_w, is

Downloaded from jer.sagepub.com at UNIV OF MICHIGAN on February 18, 2016

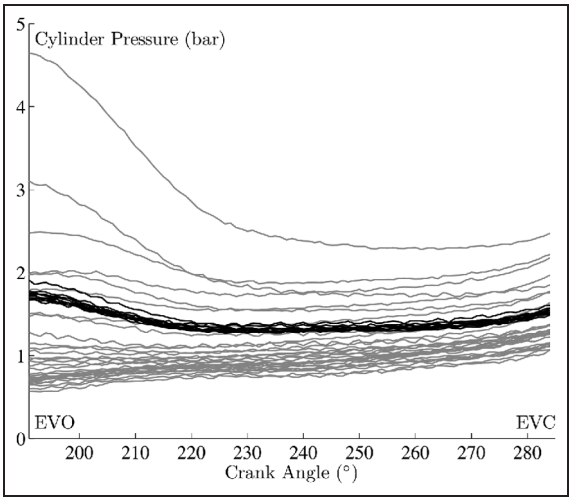

Figure 2. Minimum in the in-cylinder pressure trace can be seen to occur at EVO for some cycles in highly variable data with misfires as shown in gray. This is contrary to normal combustion, in black, where the minimum is typically close to the middle.
EVO: exhaust valve opening; EVC: exhaust valve closing.

assumed and the in-cylinder temperature, T_{cyl}, is obtained using a polytropic process. The result of equation (6) is substituted into equation (4) to yield the heat loss ratio as a function of the temperature at the valve events

$$r_{ex} = f(T_{evo}, T_{evc}) \tag{7}$$

In summary, equations (2), (5) and (7) are three equations with three unknowns T_{evo}, T_{evc} and r_{ex}. Due to the nonlinear relationship in equation (7), the solution is found numerically. For a given r_{ex}, equations (2) and (5) are solved for (T_{evo}, T_{evc}). Inserting the solutions into equation (7) gives an implicit relation that is solved numerically. The fixed-point iteration, $r_{ex}(k+1) = f(T_{evo}(r_{ex}(k)), T_{evc}(r_{ex}(k)))$, $r_{ex}(0) = 1$, was a fast method of solutions, typically only five iterations were required for convergence in most datasets with a termination condition of $|r_{ex}(k) - r_{ex}(k-1)| < 10^{-4}$. With the solution ($r_{ex}$, T_{evo}, T_{evc}), the mass of residuals may be found with the ideal gas law. The residual gas fraction is then determined by

$$x_r = \frac{m_{res}}{m_{air} + m_f + m_{res}} = \frac{P_{evc}V_{evc}T_{evo}}{P_{evo}V_{evo}T_{evc}} \tag{8}$$

Despite the fast convergence of this routine, it is too slow for implementation in an industrial engine control unit (ECU). To alleviate the need for iterations, we could instead fix the value of r_{ex} as a constant.

It can be hypothesized that the value of r_{ex} will be greater than 1. This is due to the fact that blowdown, a process in which a large amount of heat is lost due to a rapid equalization of pressure between the exhaust manifold and cylinder, occurs in the first part of the exhaust process and the fact that we have defined the two portions of equation (4) to be of equal length. The exact value of this ratio is unknown without the iterative process previously described. However, the iterative analysis supports this claim where the average value across multiple operating conditions is $r_{ex} = 1.5$. The effect of r_{ex} on the final result is small, as will be shown section "Sensitivity." It could therefore be delegated as a tuning factor; for this analysis, it is assumed a known constant.

Real-time estimation

Residual gas fraction was determined using the iterative approach in section "Iterative estimation" is suitable for offline analysis; however, the iterative nature limits its use for real-time estimation. The iterations of this algorithm were eliminated by assigning the variable r_{ex} to a fixed value. However, the method is still not suitable for real-time estimation on an actual engine because it is restricted to steady state.

In section "Iterative estimation," steady state was assumed through conservation of mass in equation (1). To provide flexibility in this assumption, the unknown temperatures of equation (2) can instead be defined with the ideal gas law

$$T_{evo} = \frac{P_{evo}V_{evo}}{m_{evo}R} \tag{9}$$

$$T_{evc} = \frac{P_{evc}V_{evc}}{m_{evc}R} \tag{10}$$

and the masses can be defined by

$$m_{evo} = m_{in}(k) + m_{res}(k) \tag{11}$$

$$m_{evc} = m_{res}(k+1) \tag{12}$$

Equation (11) tells us that the mass of charge at θ_{evo} is equal to the mass of inducted air and fuel as well as the mass of residuals from the current cycle. After the exhaust process is complete, the mass at the time of θ_{evc} is equivalent to the mass of residual trapped for the next cycle, according to the cycle definition of Figure 1. This formulation provides flexibility during non-stationary conditions as it allows m_{res} to evolve in time following real-time measurements of T_{ex} and P_{cyl}. The measurement of T_{ex} is achieved with a thermocouple in the exhaust runner port in this work. This could be replaced with a model, or a fast sensor, in future work to mitigate the potential issue of slow thermocouple response times. The in-cylinder pressure sensor, however, is capable of responding on a crank angle resolution basis. The algorithm carries a high sensitivity to P_{cyl} and a moderate sensitivity to T_{ex} as will be discussed further in section "Sensitivity."

Equations (5), (9) and (10) can then be combined and written as

$$\frac{(c_p + a)P_{evo}V_{evo}}{(m_{in}(k) + m_{res}(k))R} + \frac{(c_p - b)r_{ex}P_{evc}V_{evc}}{m_{res}(k+1)R} = T_{ex}\{c_p - a + (c_p + b)r_{ex}\} \tag{13}$$

Downloaded from jer.sagepub.com at UNIV OF MICHIGAN on February 18, 2016

Equation (13) can be written more compactly by grouping terms and lumping constant coefficients

$$m_{res}(k+1) = \frac{\alpha(k) + \beta(k) m_{res}(k)}{A(k) + m_{res}(k)} \tag{14}$$

where

$$\alpha(k) = \left(\frac{r_{ex}(b - c_p)}{c_p - a + (c_p + b) r_{ex}}\right)\left(\frac{P_{evc} V_{evc}}{R T_{ex}}\right) m_{in}(k)$$

$$\beta(k) = \left(\frac{r_{ex}(b - c_p)}{c_p - a + (c_p + b) r_{ex}}\right)\left(\frac{P_{evc} V_{evc}}{R T_{ex}}\right)$$

$$A(k) = \left(\frac{c_p + a}{c_p - a + (c_p + b) r_{ex}}\right)\left(\frac{P_{evo} V_{evo}}{R T_{ex}}\right) + m_{in}(k)$$

The values of P_x, T_x and V_x are all from the $k+1$ cycle. Equation (14) predicts the amount of residual mass in cycle $k+1$ based on previous measured data and the value of the residual mass on the previous cycle. Therefore, the only unknown is the initial guess of $m_{res}(0)$. It will be shown in the following sections that regardless of the initial guess, the difference equation will converge relatively quickly to a stable equilibrium. A limitation of the algorithm is that it requires a transient air mass as an input. Figure 1 provides a visual representation of this algorithm and its inputs relative to the cycle definition at EVO.

Undefined sets. Due to the fact that equation (14) is rational, there are sets of values (α, β, A) for which the difference equation is undefined, namely, when division by 0 occurs. The conditions are unphysical in nature; however, it is important that we consider these possibilities to understand any numerical issues that may arise. For the following analysis, r_{ex} is assumed to be equal to 1 for mathematical simplicity. Division by 0 occurs when

$$A + m_{res}(k) = 0 \rightarrow m_{res}(k) = -A$$

This scenario is obviously unphysical and can be avoided by picking a positive initial guess of residual mass. If $m_{res}(k) > 0$, then $m_{res}(k+1) > 0$; this is discussed further in section "Convergence."

Another possible numerical issue occurs when $\alpha = \beta A$. This causes a single solution for all cycles

$$m_{res}(k+1) = \frac{\beta A + \beta m_{res}(k)}{A + m_{res}(k)} = \beta \; \forall \; k \geqslant 0$$

Essentially, the algorithm could become "stuck" on this solution if there were no changes in the coefficients. However, if we evaluate the term $\alpha - \beta A = 0$, we see that for this to be true

$$\left(\frac{2c_p + R \ln\left(\frac{P_{ref}}{P_{evo}}\right)}{-4c_p + R \ln\left(\frac{P_{ref}^2}{P_{evo} P_{evc}}\right)}\right)\left(\frac{P_{evo} V_{evo}}{R T_{ex}}\right) = 0$$

Since we know the ratio inside the natural log is always close to 1, the value of the logarithm is close to 0. Additionally, $P_{evo} V_{evo}$ can never equal 0 and the value of $2c_p$ is always positive so it is unlikely this expression is ever true.

Dynamic analysis

In a stationary condition, it is important to investigate the existence of an equilibrium and the potential multiplicity issue. Additionally, it is important to understand the nature of convergence to an equilibrium for transient conditions. In the following sections, an analysis of equation (14) will be performed for which the coefficients α, β and A will be assumed constant. Specifically, a proof that equation (14) has two fixed-point solutions for a given set of inputs is provided in section "Existence of two solutions" and an analysis that shows that the algorithm converges to a physical solution is given in section "Convergence." A sensitivity analysis is performed in section "Sensitivity."

Existence of two solutions

An equation in the form of equation (14) is well known in mathematics as the Riccati difference equation, as shown in Kulenović and Ladas.[22] Since the equation is rational and of second order, it can have at most two solutions; these solutions can be real or imaginary. It is important to understand what these solutions are for a given set of input data and the stability of each solution.

To find the two solutions, we impose a change in variables such that

$$m_{res}(k) = (\beta + A) w(k) - A \; \forall \; k \geqslant 0$$

and substituting this into equation (14), we then have the difference equation

$$w(k+1) = 1 - \frac{Q}{w(k)} \quad \text{where} \quad Q = \frac{\beta A - \alpha}{(\beta + A)^2} \tag{15}$$

At steady state, $w(k+1) = w(k) = w$, the expression can be written as $w^2 - w + Q = 0$. This is an easily solved quadratic equation that yields the two possible solutions

$$w_- = \frac{1 - \sqrt{1 - 4Q}}{2} \quad \text{and} \quad w_+ = \frac{1 + \sqrt{1 - 4Q}}{2} \tag{16}$$

If $Q < 1/4$, then equation (15) has two real solutions. If $Q > 1/4$, then there are two imaginary solutions, and if $Q = 1/4$ then the solutions are $w_- = w_+ = 1/2$.

To prove this equation always has these two solutions, we can show the value of Q is less than $1/4$ and is negative for any physically reasonable set of pressure data. To do this, we examine the sign of Q. We may first exclude the denominator because it is squared and will always be positive. Therefore, the sign of Q is

Downloaded from jer.sagepub.com at UNIV OF MICHIGAN on February 18, 2016

dictated by the sign of the numerator alone. The numerator, $\beta A - \alpha$, can be rearranged as $\beta(A - m_{in}(k))$, which can be evaluated in detail as

$$\beta(A - m_{in}(k)) = \left(\frac{P_{evc}V_{evc}P_{evo}V_{evo}}{R^2T_{ex}^2}\right) \left(\frac{\left(-2c_p + R\ln\left(\frac{P_{evc}}{P_{ref}}\right)\right)\left(2c_p + R\ln\left(\frac{P_{ref}}{P_{evo}}\right)\right)}{\left(-4c_p + R\ln\left(\frac{P_{ref}^2}{P_{evo}P_{evc}}\right)\right)^2}\right)$$

From this, we can see that the sign of Q is determined by

$$\left(-2c_p + R\ln\left(\frac{P_{evc}}{P_{ref}}\right)\right)\left(2c_p + R\ln\left(\frac{P_{ref}}{P_{evo}}\right)\right)$$

since the term $(P_{evc}V_{evc}P_{evo}V_{evo})$ is always positive. Expansion of terms yields

$$-4c_p^2 + 2c_pR\ln\left(\frac{P_{evc}P_{evo}}{P_{ref}^2}\right) + R^2\ln\left(\frac{P_{evc}}{P_{ref}}\right)\ln\left(\frac{P_{ref}}{P_{evo}}\right) \quad (17)$$

The sign of this term dictates the sign of Q. To find the sign of this term, we must apply some constraints on the pressures. We know during the exhaust process P_{evo}, P_{evc} and P_{ref} are all very close to one another, therefore

$$\frac{P_{evc}P_{evo}}{P_{ref}^2} \approx \frac{P_{evc}}{P_{ref}} \approx \frac{P_{ref}}{P_{evo}} \approx 1$$

Because of this, the last two terms of equation (17) are very close to 0 and are small by comparison to the first term, which is always negative. In fact, for equation (17) to become positive, the pressure ratios inside the natural logs would all have to be greater than 20. Since exhaust pressures are usually around 1 bar and not more than 5 bar for most applications, pressure ratios of this magnitude are not feasible. We can therefore conclude the sign of Q is always negative for physically reasonable data and there will always be two solutions, w_- and w_+, given by equation (16). Using this same argument, we can support the claim in section "Real-time estimation" that $\alpha - \beta A$ is not equal to 0. The preceding argument shows $\beta A - \alpha$ is always less than 0.

Convergence

Equation (14) predicts the amount of residual mass in cycle $k + 1$ based on measured data and the value of the residual mass in the previous cycle. Therefore, the only unknown is the initial guess of $m_{res}(0)$. Since we know the equation has two fixed-point solutions, as shown in section "Existence of two solutions," it is desirable to know how the equation converges to these solutions and if the solutions are stable.

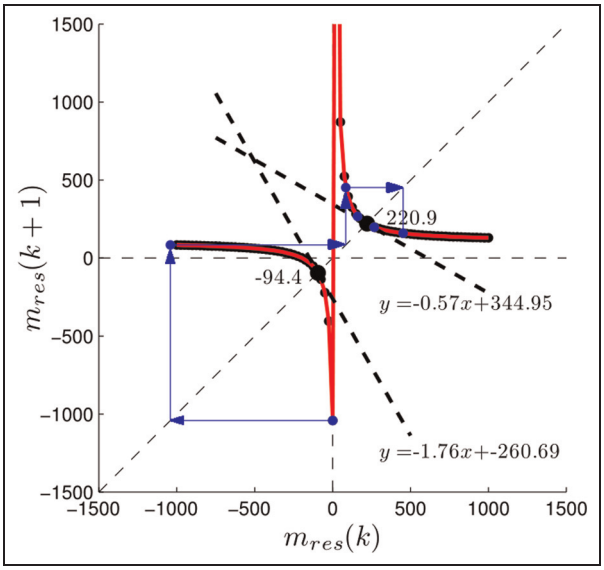

Figure 3. Change in the value of the estimated m_{res}, in milligrams, from one cycle to the next. Two fixed-point solutions are shown and the slop at each point indicates the solutions stability.

If typical values of α, β and A are used in the residual mass estimation and held constant, the change from one cycle to the next can be determined from the discrete derivative of equation (14).

An example of this is shown in Figure 3 for initial conditions ranging from −1000 to 1000 mg. Here, the equation has equilibria at −94.4 and 220.9 mg. Clearly, the negative solution is non-physical as we cannot have a negative mass. If we linearize the function at each one of the equilibria, we find that the slope at the negative solution is outside the criteria for a stable equilibrium. Specifically, if the solution was stable, the slope at the solution would be $-1 < m < 1$, where m is the slope of the function at a particular point. The slope at the positive solution is −0.57, and this equilibrium is therefore stable and oscillatory. As such, an initial condition that is close to stable equilibria will converge to the positive solution for this set of coefficients. The figure shows how an initial guess of $m_{res}(0) = 0$ would converge to the stable equilibrium in blue. Further stability properties of the Riccati difference equation can be found in Kulenović and Ladas,[22] Grove et al.[23] and Sedaghat.[24]

Figure 4 highlights the evolution of convergence from various positive initial guesses. In this case, the initial guess was purposely chosen to be far away from the actual value to demonstrate the nature of convergence at various conditions. In real operation, the initial guess is chosen to be more physically reasonable and close to the actual value. It can be seen here that the equation converges to the same predicted residual mass within a small number of cycles. Additionally, it converges to approximately the same value as a higher fidelity offline analysis tool.[15]

Downloaded from jer.sagepub.com at UNIV OF MICHIGAN on February 18, 2016

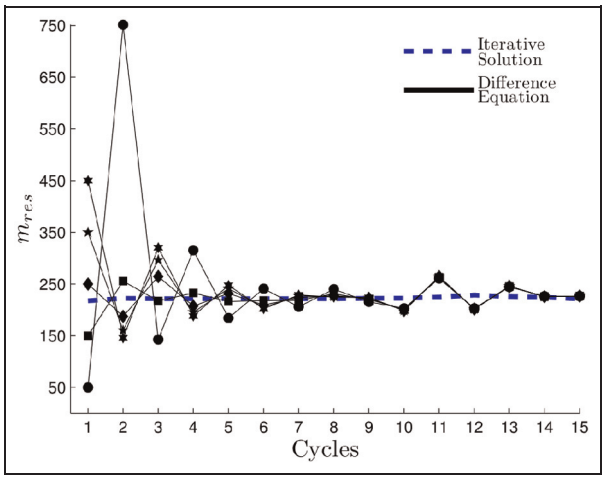

Figure 4. Convergence of the state m_{res}, in milligrams, from various initial guesses. Simulation was run using experimental data at 1800 r/min, 3 bar IMEP and a combustion phasing of 8° after top dead center.
IMEP: indicated mean effective pressure.

Sensitivity

In the preceding analysis, the heat loss ratio r_{ex} was assumed to be 1 for mathematical simplicity. However, it will most likely always be greater than 1. To better understand the influence that this parameter has on the residual mass estimate, an analysis was done in which the state was allowed to converge to steady state for a guess of $m_{res}(0) = 250$ mg and for values of r_{ex} ranging from 0.75 to 2. The result can be found in Figure 5. Here, it can be seen that the positive solution (w_+) is mostly insensitive for values of r_{ex} greater than 1. A change of approximately 1 mg is observed from $r_{ex} = 1 \rightarrow 2$. Therefore, due to the insensitivity, it is a valid assumption to allow this parameter to stay constant. It could also be tuned to offline data analysis results. For the data presented in Figure 7, the average value from offline analysis was found to be $r_{ex} = 1.5$.

Figure 5 shows the sensitivity of the unphysical solution (w_-) to the heat loss ratio. This solution does have a high sensitivity; however, as r_{ex} is increased, the solution becomes more negative. It can also be seen how the slope of the function changes at these two equilibria. For the positive solution, the slope remains stable. The unphysical solution is persistently unstable.

Since the residual estimation state depends on measurements of the exhaust gas temperature and fresh air mass, it is important to determine the sensitivity of the equation to these parameters. Figure 5 also shows how the residual mass changes as a function of an error in the measurement of exhaust gas temperature and fresh air mass. The effect of these errors is approximately affine and relatively flat, indicating moderate sensitivity. The result is more linear and less sensitive for a heat loss ratio greater than 1.

In summary, the steady-state value of the residual estimation is relatively insensitive to the heat loss ratio r_{ex}. However, the heat loss ratio does have an effect on the dynamics and convergence properties. Also, there are moderate sensitivities to errors in the measure exhaust gas temperature and inducted air mass. The estimation routine carries its highest sensitivity to the measured in-cylinder pressure which can be obtained at high speed with good measurement accuracy.

Experimental results and setup

A four-cylinder 2-L General Motors LNF Ecotec engine with direct injection is used as the baseline platform, see Figure 6. EPA Tier III Certification fuel was used for all tests. To accommodate HCCI combustion, the compression ratio was raised to 11.25:1 and camshafts with shorter duration and lower lift were used to allow for unthrottled operation. A small supercharger (Eaton M24) was added to the air path in series with the stock turbocharger to provide additional boosting capabilities. Engine coolant temperature was controlled to a set-point of 90 °C for all tests. The spark was left on, but at a position of 40° after top dead center (aTDC). The mixture is lean and highly diluted with residuals for the tests in this work, and as such the spark will have little influence on the combustion. Having the spark on late only helps to prevent the plug from fouling.

Cylinder pressures were sampled at a resolution of 0.1° crank angle degree (CAD) for offline pressure analysis; however, real-time estimation of combustion features was done at a resolution of 1° CAD. The estimation algorithm was implemented using a combination of C and MATLAB code and was tested in real-time using an ETAS ES910 rapid prototyping module. The module uses an 800 MHz Freescale™ PowerQUICC III MPC8548 processor with double-precision floating point arithmetic and 512 MB of RAM. In the experiments presented here, the air and fuel masses used for real-time residual estimation were found using manifold filling dynamics, a cylinder filling model and a torque estimation model on the Bosch Motronic ECU. The models used for air and fuel mass determination are computationally simple and use only production sensors as they must run in real-time on the ECU, which is intended for production and is very limited in computation capacity. The model for air charge determination is calibrated with experimental data to ensure accurate estimation. As discussed in section "Sensitivity," equation (14) carries a moderate sensitivity to the value of inducted air mass, as such it is important to have an accurate model, or sensor, for this input. Examples of air charge determination models can be found in Rausen et al.[25] and Buckland et al.[26] For offline analysis, the air and fuel masses are determined through post-processing of data from several sensors. The offline determination of air charge is, in general, more accurate than the cylinder filling model from the Bosch ECU.

Downloaded from jer.sagepub.com at UNIV OF MICHIGAN on February 18, 2016

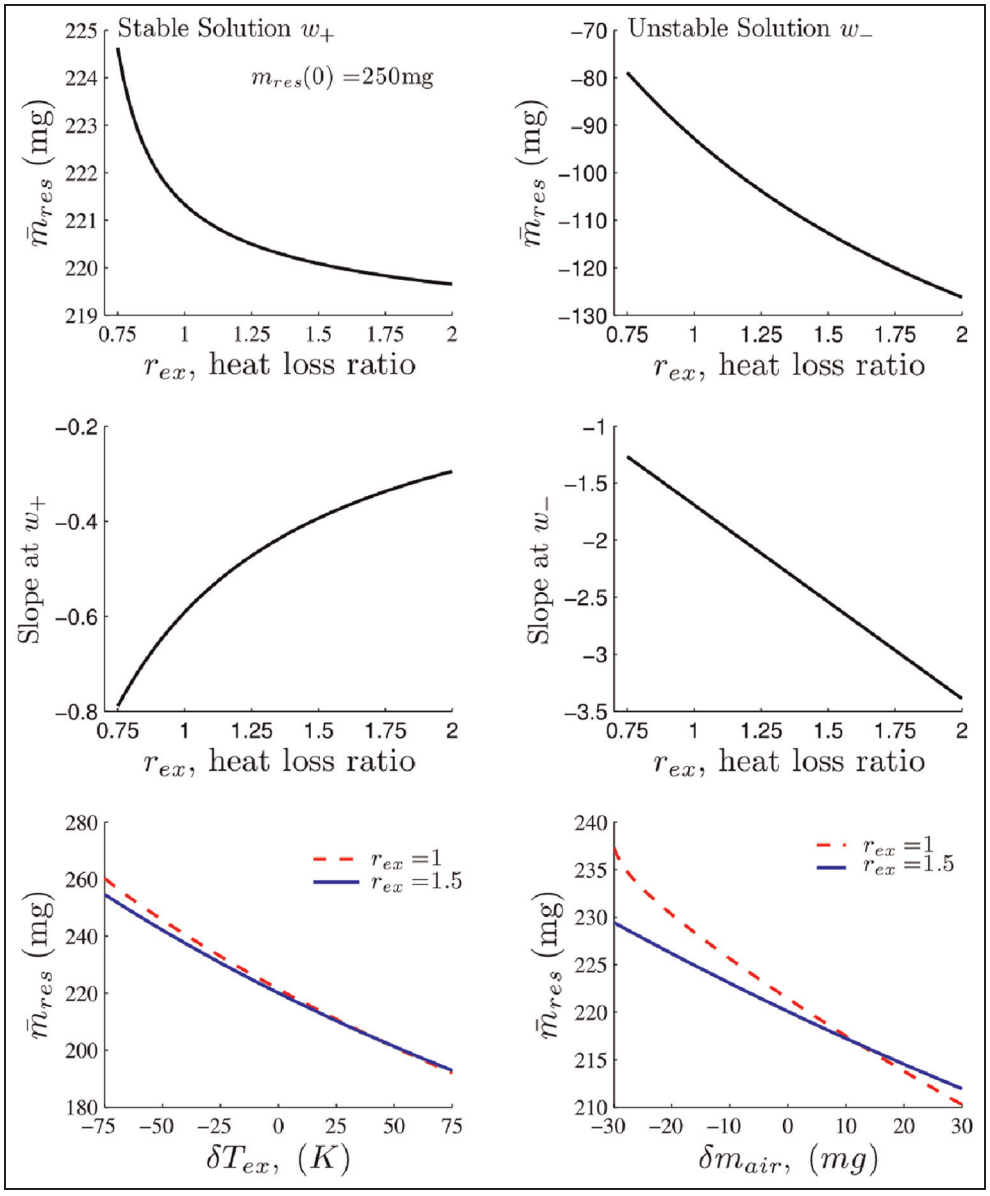

Figure 5. Sensitivity of the residual mass to errors in the measured exhaust gas temperature. The sweeps are performed for various heat loss ratios, and the results are linear for a physically reasonable value of r_{ex}.

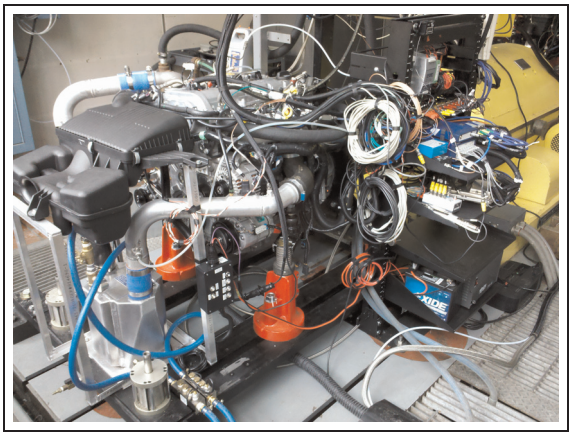

Figure 6. Multicylinder recompression HCCI engine used for testing along with all rapid prototyping hardware and instrumentation.

Comparison to steady-state data

To validate the online residual estimation's accuracy, it was compared to the results from the offline estimation presented in section "Iterative estimation." Ideally, the results from the online analysis would be compared against measurements of the residual mass. Unfortunately, sampling of the in-cylinder charge is extremely difficult; it has, however, been done in Steeper and Davisson.[27] This method, however, requires steady-state operation and the engine cannot continue to run once a sample has been taken.

The dataset used for comparison spans multiple speeds, loads and actuator settings and is therefore representative of the range of inputs that the equation would receive when operating online. The results in Figure 7 show that for values of $r_{ex} = 1$, the fit is good

Downloaded from jer.sagepub.com at UNIV OF MICHIGAN on February 18, 2016

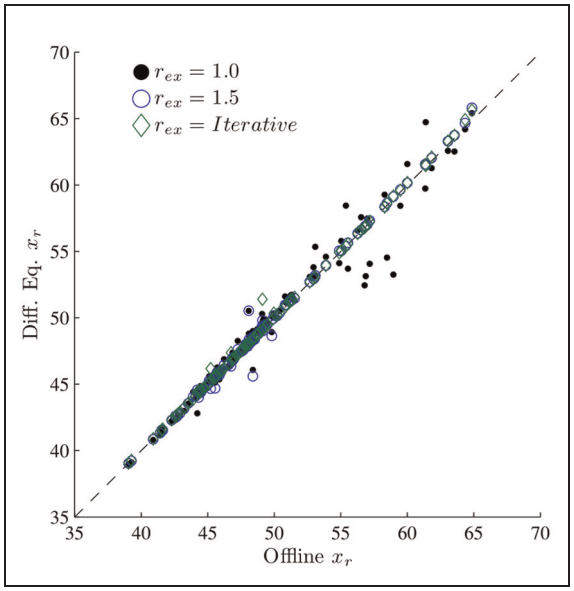

Figure 7. Comparison of the online residual estimation with that of an iterative offline analysis tool from Fitzgerald et al.[15].

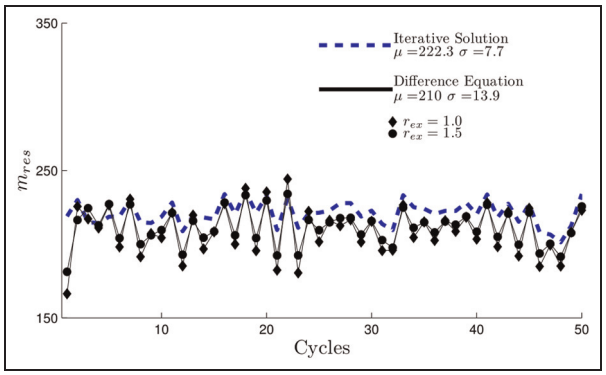

Figure 8. Cycle-resolved results of residual mass for different values of r_{ex}. Despite the data's high variability, the algorithm captures cycle-by-cycle trends well. The increased value of r_{ex} dampens oscillations.

with the exception of a few outliers. The outliers correspond to higher load points. For these, the pressure in the cylinder at the point of EVO was high due to higher peak pressures. The result is a larger blowdown event which would make the value of r_{ex} necessarily greater than 1. The results are better when a heat loss ratio greater than 1 is used and nearly identical to the offline analysis when the value of r_{ex} from the iterative method is used. This comparison of the data was made offline.

Cycle-by-cycle trends

Since the residual mass trapped in the cylinder can change quickly on a cycle-by-cycle basis, it is important to quantify how well the algorithm can capture these fluctuations. Figure 8 shows the result of the online difference equation and offline analysis for a highly variable dataset. These data were made variable by reducing the amount of NVO and therefore trapped residual mass such that the combustion phasing became sufficiently late to induce oscillations in the combustion phasing and cylinder pressure.[14] Figure 8 shows that the online estimation well approximates the offline result in terms of direction of change from one cycle to the next in the presence of this high variability in P_{cyl}. However, it is possible that in the extreme vase of frequent misfires that the algorithm could saturate and have difficulty converging back to a solution.

The standard deviation of the online result is higher than that of the offline. This is due to the oscillatory convergence of the online estimation. When a heat loss ratio greater than 1 is used, the amplitude of oscillations is reduced. This is the same result deduced from Figure 5 where we see that the slope of the function at the physical solution is approaching 0 as the heat loss ratio is increased. This slope is analogous to the eigenvalue of the system. In discrete time, an eigenvalue on the left-half plane and inside the unit circle is stable but oscillatory. As we move the eigenvalue closer to positive values, the dampening of the system increases. Additionally, errors could result from the different means by which the cycle-by-cycle air mass is determined. For the online solution, the air mass is determined using the Bosch ECU and a cylinder filling model as outlined in section "Experimental results and setup."

To further check the statistical properties of the algorithm, we consider the full test from Figure 8 which is 3000 cycles long. The results are presented in Figure 9 with return maps and normal probability plots. A return map shows the relationship between consecutive cycles which provides insight on the dynamic behavior of the cyclic variability (CV). Here, the return map is the plot of the residual mass in cycle k versus the residual mass in cycle $k + 1$. When comparing the online and offline results, we can see that the online analysis results are stretched slightly perpendicular to the diagonal indicating oscillatory behavior. This is most likely caused by the heat loss ratio being tuned slightly low as previous results would indicate. The results for both cases are mostly Gaussian as indicated by the normal probability plots.

Even though the residual gas fraction data in Figure 9 appears to have fairly low variability, the effect on the combustion is actually significant and non-Gaussian. This is made clear by the return maps of combustion phasing and heat release in Figure 10.

Actuator steps

To evaluate the effectiveness of the residual gas fraction estimation in transients, actuator steps of the model inputs were performed in open loop. Sensor measurements were obtained in real-time from the engine's ECU and used by the model for real-time prediction of x_r. A step in EVC is shown in Figure 11 for cylinder 1. The step is from 256° to 253° aTDC and back again

Downloaded from jer.sagepub.com at UNIV OF MICHIGAN on February 18, 2016

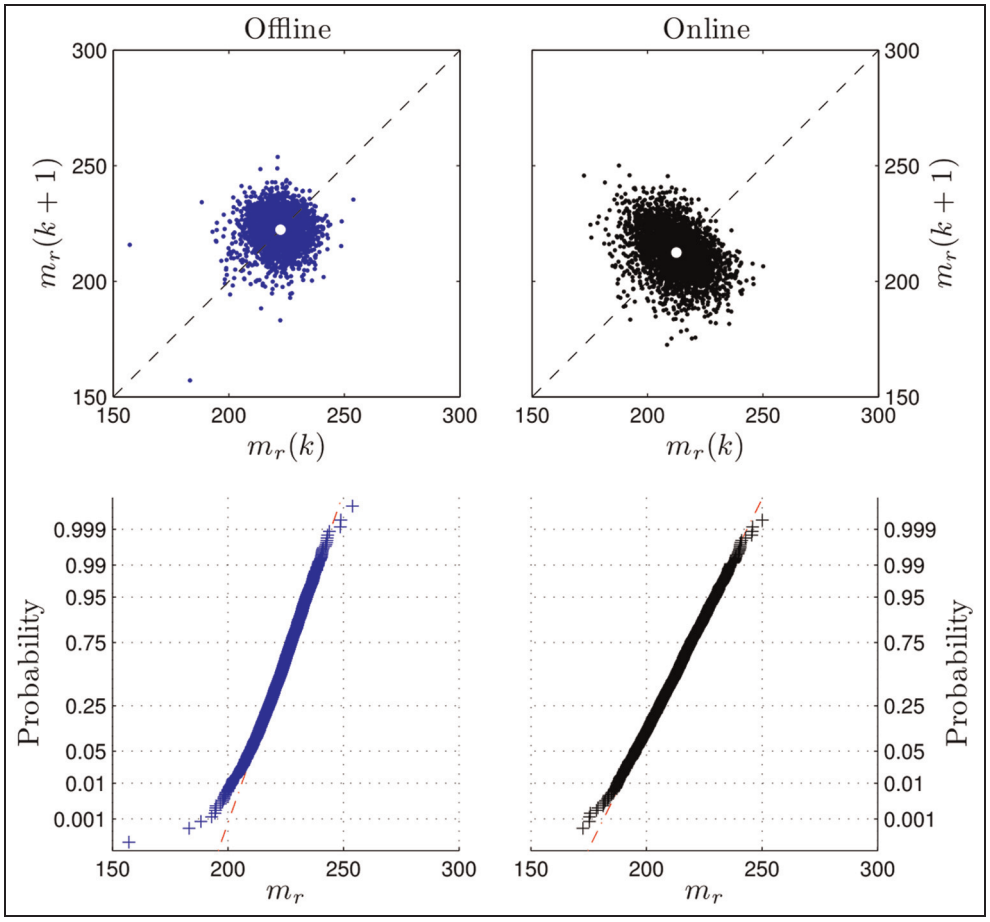

Figure 9. Return maps and normal probability plots of the online and offline residual estimation for a highly variable dataset.

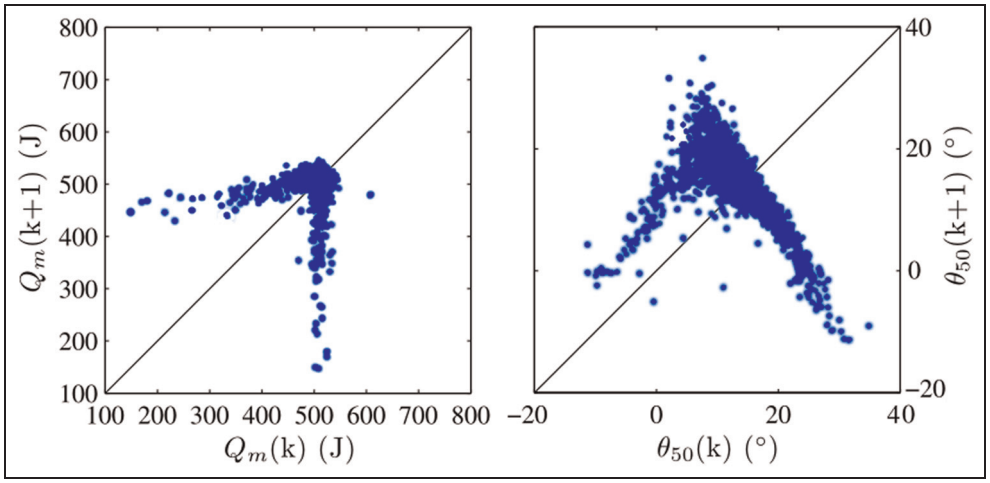

Figure 10. Return maps of heat release and combustion phasing for the data presented in Figure 9. Here, it can be seen that despite the low variability in the return maps of residual gas fraction, the combustion is erratic in terms of θ_{50} and heat release.

and causes the amount of NVO to increase as a result. Intuitively, the amount of residual mass trapped in the cylinder should also increase; this is reflected in the prediction of the residual gas fraction. The EVC step is small because this is the largest step change that can be achieved in open loop at this particular operating condition. Without compensation from other actuators, the engine transitions between nearly misfiring and ringing with this slight change in residual gas fraction as seen by the response of combustion phasing in Figure 11. Also shown is the result of the offline analysis of the residual gas fraction from Fitzgerald et al.[15] and Larimore et al.[19] While the absolute difference between the two results is not 0, the magnitude and

Downloaded from jer.sagepub.com at UNIV OF MICHIGAN on February 18, 2016

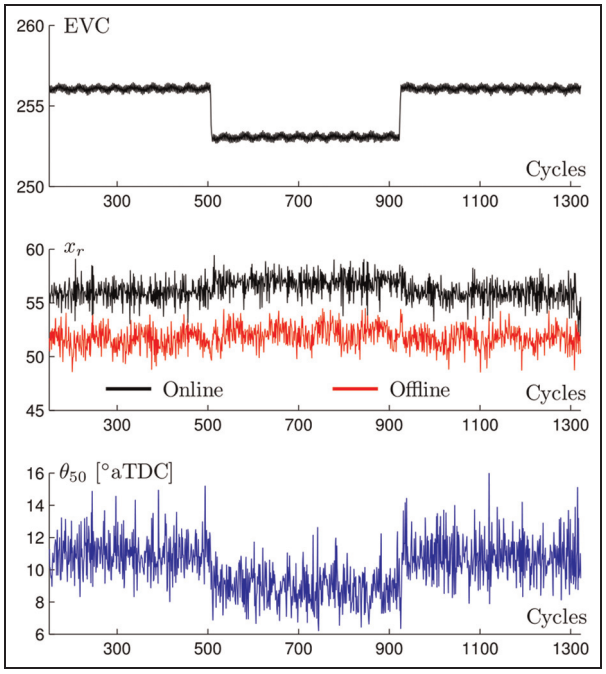

Figure 11. An EVC step for cylinder 1. The online residual gas fraction prediction (black) is compared against the offline prediction (red). The cycle-by-cycle predictions are good throughout the test; however, there is an offset in the mean value most likely caused by a difference in the estimation of mass of air. The step is small because an open-loop EVC step has a large effect on the combustion phasing.
EVC: exhaust valve closing; aTDC: after top dead center.

direction of the transient response are similar. The absolute value of the two results differs due to the different methods used to calculate the inducted air mass as discussed in section "Experimental results and setup."

Conclusion

A physics-based method of estimating the trapped residual mass in a recompression engine using cylinder pressure measurements has been presented and evaluated through dynamic analysis and experiments. An accurate estimation of residual mass is important to understand and control HCCI dynamics due to its large sensitivity to thermal properties of the charge mass. In recompression HCCI, the charge temperature is most directly effected by the trapped residual mass.

The algorithm is viable for real-time implementation due to its simplicity and it has been shown that the estimation is valid for highly variable datasets. This is due to the algorithm's ability to converge quickly from perturbations. Furthermore, an analysis has been done to show sensitivity properties to a tuning parameter and measurement errors. The tuning parameter r_{ex} has little influence on the steady-state result but does impact the dynamics and convergence of the algorithm. A limitation of the algorithm is that it requires a transient air mass as an input. The results from the residual estimation are sensitive to errors in this input as indicated by Figure 5 and so it is imperative that a well-parameterized charge determination model is used when implementing the algorithm online.

Declaration of conflicting interests

This report was prepared as an account of work sponsored by an agency of the US Government. Neither the US Government nor any agency thereof, nor any of their employees, makes any warranty, express or implied, or assumes any legal liability or responsibility for the accuracy, completeness, or usefulness of any information, apparatus, product, or process disclosed, or represents that its use would not infringe privately owned rights. Reference herein to any specific commercial product, process, or service by trade name, trademark, manufacturer, or otherwise does not necessarily constitute or imply its endorsement, recommendation, or favoring by the US Government or any agency thereof. The views and opinions of authors expressed herein do not necessarily state or reflect those of the US Government or any agency thereof.

Funding

This material was supported by the Department of Energy (National Energy Technology Laboratory) DE-EE0003533 as a part of the ACCESS project consortium with direction from Hakan Yilmaz and Oliver Miersch-Wiemers, Robert Bosch, LLC.

References

1. Olsson JO, Tunestål P and Johansson B. Closed-loop control of an HCCI engine. SAE paper 2001-01-1031, 2001.
2. Shaver GM and Gerdes JC. Cycle to cycle control of HCCI engines. In: *Proceedings of IMECE* 2003, Washington, DC, 15–21 November 2003, IMECE2003-41966. ASME Technical Publishing Office, NY.
3. Yao M, Zheng Z and Liu H. Progress and recent trends in HCCI engines. *Prog Energ Combust* 2009; 35(5): 398–437.
4. Willand J, Nieberding RG, Vent G and Enderle C. The knocking syndrome—its cure and its potential. SAE paper 982483, 1998.
5. Roelle MJ, Jungkunz AF, Ravi N and Gerdes JC. A dynamic model of recompression HCCI combustion including cylinder wall temperature. In: *Proceedings of IMECE 2006*, Chicago, IL, 5–10 November 2006, IMECE2006-15125. ASME Technical Publishing Office, NY.
6. Wermuth N, Yun H and Najt P. Enhancing light load HCCI combustion in a direct injection gasoline engine by fuel reforming during recompression. *SAE Int J Engines* 2009; 2: 823–836.
7. Marriott C and Reitz R. Experimental investigation of direct injection-gasoline for premixed compression ignited combustion phasing control. SAE paper 2002-01-0418, 2002.
8. Chiang CJ and Stefanopoulou AG. Stability analysis in homogeneous charge compression ignition (HCCI)

Downloaded from jer.sagepub.com at UNIV OF MICHIGAN on February 18, 2016

engines with high dilution. *IEEE T Contr Syst T* 2007; 15(2): 209–219.
9. Daw CS, Wagner RM, Edwards KD Jr and Johney BGJr. Understanding the transition between conventional spark-ignited combustion and HCCI in a gasoline engine. *P Combust Inst* 2007; 31(2): 2887–2894.
10. Kulzer A, Lejsek D, Kiefer A and Hettinger A. Pressure trace analysis methods to analyze combustion features and cyclic variability of different gasoline combustion concepts. SAE paper 2009-01-0501, 2009.
11. Shahbakhti M and Koch CR. Characterizing the cyclic variability of ignition timing in a HCCI engine fueled with n-heptane/iso-octane blend fuels. *Int J Engine Res* 2008; 9(5): 361–397.
12. Manofsky L, Vavra J, Assanis D and Babajimopoulos A. Bridging the gap between HCCI and SI: spark-assisted compression ignition. SAE paper 2011-01-1179, 2011.
13. Hellström E, Stefanopoulou AG and Jiang L. Cyclic variability and dynamical instabilities in autoignition engines with high residuals. *IEEE T Contr Syst T* 2013; 21(5): 1527–1536.
14. Hellström E, Larimore J, Sterniak J, Jiang L and Stefanopoulou A. Quantifying cyclic variability in a multicylinder HCCI engine with high residuals. *J Eng Gas Turb Power* 2012; 134: 112803.
15. Fitzgerald RP, Steeper R, Snyder J, Hanson R and Hessel R. Determination of cycle temperature and residual gas fraction for HCCI negative valve overlap operation. *SAE Int J Engines* 3: 124–141 (2010-01-0343).
16. Mladek M and Onder C. A model for the estimation of inducted air mass and the residual gas fraction using cylinder pressure measurements. *SAE Int* 2000; 1: 1–11 (2000-01-0958).
17. Gazis A, Panousakis D, Patterson J, Chen HW, Chen R and Turner J. Using in-cylinder gas internal energy balance to calibrate cylinder pressure data and estimate residual gas amount in gasoline HCCI combustion. *Exp Heat Transfer* 2008; 21(4): 275–280.
18. Ortiz-Soto EA, Vavra J and Babajimopoulos A. Assessment of residual mass estimation methods for cylinder pressure heat release analysis of HCCI engines with negative valve overlap. In: *Proceedings of ASME 2011 internal combustion engine division fall technical conference*, Morgantown, WV, 2–5 October 2011. ASME Technical Publishing Office, NY.
19. Larimore J, Hellström E, Sterniak J, Jiang L and Stefanopoulou A. Experiments and analysis of high cyclic variability at the operational limits of spark-assisted HCCI combustion. In: *Proceedings of the American control conference (ACC)*, Montréal, QC, Canada, 27–29 June 2012, pp.2072–2077. New York: IEEE.
20. Hellström E, Stefanopoulou AG, Vavra J, Babajimopoulos A, Assanis D, Jiang L and Yilmaz H. Understanding the dynamic evolution of cyclic variability at the operating limits of HCCI engines with negative valve overlap. *SAE Int J Engines* 2012; 5(3): 995–1008.
21. Heywood J. *Internal combustion engine fundamentals*. McGraw-Hill Science/Engineering/Math, 1988, NY.
22. Kulenović MRS and Ladas G. *Dynamics of second order rational difference equations with open problems and conjectures*. Boca Raton, FL: Chapman and Hall/CRC, 2002.
23. Grove EA, Ladas G, McGrath LC and Teixeira CT. Existence and behavior of solutions of a rational system. *Commun Appl Nonlin Anal* 2001; 8(1): 1–25.
24. Sedaghat G. Existence of solutions of certain singular difference equations. *J Differ Equ Appl* 2000; 6(5): 535–561.
25. Rausen DJ, Stefanopoulou AG, Kang JM, Eng JA and Kuo TW. A mean value model for control of HCCI engines. *J Dyn Syst: T ASME* 2005; 127(3): 355–362.
26. Buckland J, Jankovic M, Grizzle J and Freudenberg J. Estimation of exhaust manifold pressure in turbocharged gasoline engines with variable valve timing. In: *Proceedings of dynamic systems and control conference*, Ann Arbor, MI, 20–22 October 2008. ASME Technical Publishing Office, NY.
27. Steeper RR and Davisson ML. Analysis of gasoline negative-valve-overlap fueling via dump sampling. *SAE Int J Engines* 2014; 7: 762–771 (2014-01-1273).

Downloaded from jer.sagepub.com at UNIV OF MICHIGAN on February 18, 2016